LETTER • OPEN ACCESS

Integrated Joule switches for the control of current dynamics in parallel superconducting strips

To cite this article: A Casaburi *et al* 2018 *Supercond. Sci. Technol.* **31** 06LT01

View the article online for updates and enhancements.

Related content

Recent citations

IOP ebooks™

Bringing you innovative digital publishing with leading voices to create your essential collection of books in STEM research.

Start exploring the collection - download the first chapter of every title for free.

Letter

Integrated Joule switches for the control of current dynamics in parallel superconducting strips

A Casaburi[1] , **R M Heath**[1], **R Cristiano**[2], **M Ejrnaes**[2] , **N Zen**[3],
M Ohkubo[3] **and R H Hadfield**[1]

[1] School of Engineering, University of Glasgow, Glasgow, G12 8LT, United Kingdom
[2] CNR—Istituto SPIN Pozzuoli, I-80078, Pozzuoli (Napoli), Italy
[3] National Institute of Advanced Industrial Science and Technology (AIST), 1-1-1 Umezono, Tsukuba, Ibaraki 305-8568, Japan

E-mail: alessandro.casaburi@glasgow.ac.uk

Abstract
Understanding and harnessing the physics of the dynamic current distribution in parallel superconducting strips holds the key to creating next generation sensors for single molecule and single photon detection. Non-uniformity in the current distribution in parallel superconducting strips leads to low detection efficiency and unstable operation, preventing the scale up to large area sensors. Recent studies indicate that non-uniform current distributions occurring in parallel strips can be understood and modeled in the framework of the generalized London model. Here we build on this important physical insight, investigating an innovative design with integrated superconducting-to-resistive Joule switches to break the superconducting loops between the strips and thus control the current dynamics. Employing precision low temperature nano-optical techniques, we map the uniformity of the current distribution before- and after the resistive strip switching event, confirming the effectiveness of our design. These results provide important insights for the development of next generation large area superconducting strip-based sensors.

Keywords: superconducting detectors, superconducting nano-strip, ion detectors, particle detectors, TOF-MS

(Some figures may appear in colour only in the online journal)

1. Introduction

The interplay between the superconducting state and magnetic fields is a subtle and challenging problem which has been studied for more than a century. The magnetic penetration depth, λ, is the characteristic length scale over which a magnetic field penetrates into a superconducting strip and governs the flow and distribution of current [1]. For ultrathin films, with thickness $d < \lambda$, the Pearl effect becomes important and increases the characteristic length scale to $\Lambda_P = 2\lambda_2/d$ [2]. If Λ_P is comparable or smaller than the strip width, the current density will be strongly non-uniform and will decay towards zero from the edge

to inner part of the strip, in accordance with the generalized London model [1]. Recent studies show that non-uniform current distribution, in a discrete form, is also observed in blocks of N parallel connected strips when the total width of the block is comparable to or greater than Λ_P [3, 4]. In particular, it has been observed that a symmetric and non-uniform current distribution is established stably among the parallel strips just after their current biasing [3]. Also, temporary switching of individual strips into the resistive state generates vorticity, that is trapped as magnetic flux quanta in the superconducting loops of the parallel strips, in turn changing the non-uniform current distribution [4]. The current non-uniformity strongly degrades the performance
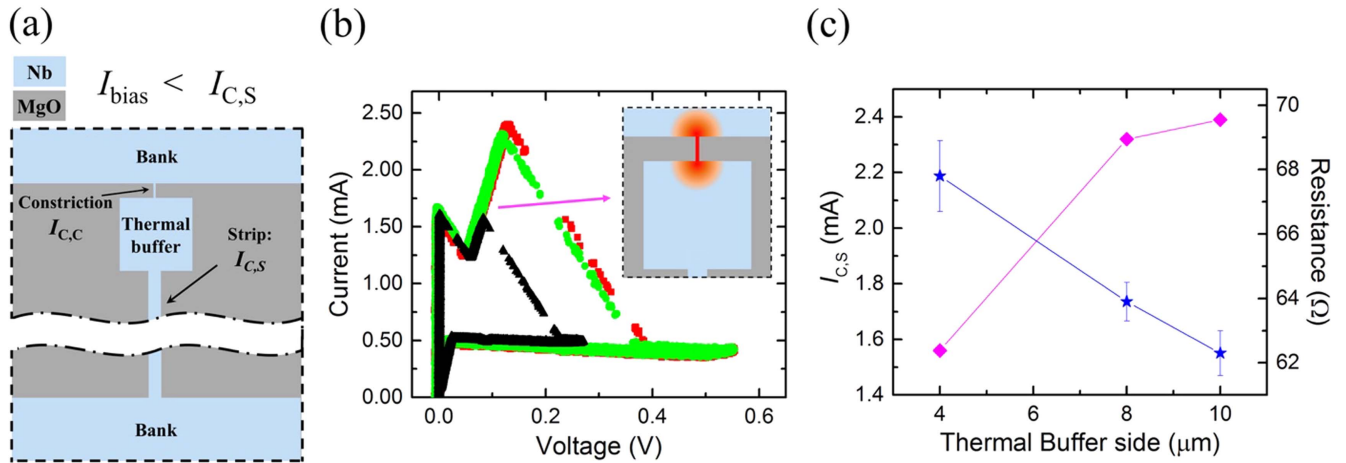
Figure 1. (a) Sketch of the proposed design for the single strip connected to the constrictions via a superconducting thermal buffer. (b) Graph showing the I–V characteristic, measured at a temperature of 4.2 K, for the strips having thermal buffer area of $4 \times 4 \ \mu m^2$ (black triangles), $8 \times 8 \ \mu m^2$ (green circles) and $10 \times 10 \ \mu m^2$ (red squares). The inset illustrates the propagation of the normal resistive region in the thermal buffer when a bias current is in the range $I_{C,C} < I_B < I_{C,S}$. (c) Graph showing the values of the measured $I_{C,S}$ (magenta diamonds) and of the resistances when the strips are biased in the range $I_{C,C} < I_B < I_{C,S}$ (blue stars) as the thermal buffer side width varies.

of superconducting strip-based detectors such as superconducting strip ion detectors (SSIDs) [5], or superconducting nanowire single photon detectors (SNSPDs) [6, 7], that use the parallel design to increase the sensitive area and retain at the same time their characteristic ultrafast response time [8–10]. The detection efficiency of SSIDs and SNSPDs increases as the current flowing in the strip rises [11, 12] and middle strips in the parallel blocks could be not sufficiently biased for efficient detection [3, 4], reducing the overall efficiency. Also, the non-uniform current distribution, occurring in the strips after a detection event [4], could trigger the cascade switch at a current lower than the threshold with consequent latching [13, 14] and instability in operation [15, 16]. This explains the poor improvement observed in the counting efficiency of a 2×2 mm^2 area SSID [17] compared with that of the four-times smaller sensitive area device of [18, 19]. Therefore, to scale up the area of SSIDs to the required size of $\sim$cm^2 and at the same time retain an ultrafast response time and high counting efficiency [10], it is necessary to understand and control the current dynamics in the parallel strips. Attempts at implementation of series resistors to the strips have been made using non superconducting elements which require impractical extra fabrication steps or the use of off-chip components [9, 20].

In this letter, we build on recent insights into the underlying device physics and propose an innovative design for breaking the superconducting loops formed from the parallel strips thus obtaining a uniform current distribution across them.

2. Superconducting constriction as bi-stable Joule switch

The main concept proposed here is to connect each superconducting strip in series with a superconducting constriction, or Joule switch, which acts as a current-controlled bi-stable resistor (figure 1(a)). The constriction has a critical current,

$I_{C,C}$, lower than the critical current of the strip, $I_{C,S}$. In this way, the resulting I–V characteristic will show superconducting behavior when the bias current $I_B < I_{C,C}$ and above this point the constriction will switch to the normal resistive state. The Joule heating will create a self-sustained hotspot in the constriction having a resistance R_C [21] whether the strip is still superconducting if $I_{C,C} < I_B < I_{C,S}$, mimicking a resistor connected in series with the single strip [20, 21]. Although is part of the same superconducting thin film layer, the constriction will interrupt the superconducting path once biased above $I_{C,C}$. Therefore, identical resistances will interrupt the superconducting loops formed by parallel connected strips allowing for a uniform current distribution according to Ohm's law. The magnetic field can move through the loops preventing the non-uniform current distribution observed in the previous experiments due to the trapping of magnetic flux and vorticity [3, 4].

Since the constriction dissipates heat during operation we must distance it thermally from the strip to avoid degrading $I_{C,S}$. We accomplish this by placing superconducting thermal buffers between the constriction and the strip (figure 1(a)). In order to choose the appropriate size for the thermal buffers, we fabricated several strips connected to a constriction via superconducting thermal buffers with area varying from $4 \times 4 \ \mu m^2$ to $10 \times 10 \ \mu m^2$ and measured $I_{C,S}$ (see figure 1(b)). The strips have all width, $W = 1 \ \mu m$ and length, $L = 500 \ \mu m$ and the constrictions have all width, $w = 250$ nm and a length, $l = 2 \ \mu m$, respectively. The structures were fabricated by patterning the 40 nm thick superconducting Nb film by a single electron beam lithography (EBL) and reactive ion etching (RIE) step. As expected, the value of $I_{C,C} \approx 1.6$ mA is almost identical whether the values of $I_{C,S}$ increase with the size of the thermal buffers (figure 1(c)). From a linear fit of the I–V curves, in the resistive region for $I_{C,C} < I_B < I_{C,S}$, it can be also seen that the resistance decreases when the size of the thermal buffer increases (figure 1(c)). This means that the resistive region is expanding

beyond the constriction edge in the thermal buffer, toward the strips, increasing the local temperature and degrading its $I_{C,S}$ (see inset figure 1(b)), according to the model of the self-heating hotspot propagating in a superconducting short bridge described in [21] for $l/\eta \approx 1$ and $w/\eta < 0.1$–0.2. In the formula, the thermal healing length is equal to $\eta \approx 1\,\mu$m and it was obtained by estimating the thermal conductivity of the Nb thin film $K \sim 0.0056\,\mathrm{W\,cm^{-1}\,K^{-1}}$ from the Weidmann–Franz law and using a value of the coefficient heat transfer per unit are to the substrate $\alpha \sim 2\,\mathrm{W\,cm^{-2}\,K^{-1}}$ [21, 22]. The resistive region would extend outside the constriction over a length of several thermal healing length η [21]. We concluded from the measured relative increases in $I_{C,S}$ between the devices, that a thermal buffer of $20 \times 20\,\mu\mathrm{m}^2$ area should be sufficiently large to prevent the degradation of $I_{C,S}$.

The return current of the strip, i.e. the minimum current to sustain the resistive state before switching to superconducting state, is $I_{\mathrm{ret,S}} \approx 0.5\,\mathrm{mA}$ (see figure 1(b)). This value is larger than the return current of the constriction $I_{\mathrm{ret,c}} \approx 0.1\,\mathrm{mA}$ (not visible on the plot scale). This is in agreement with the model of [21] which finds $I_{\mathrm{ret,S}}/I_{\mathrm{ret,c}} \geqslant 1$ obtained for $l/\eta \approx 1$ and $w/\eta < 0.1$–0.2 as in our case. Moreover, the part of the I–V curve where the constriction is in the resistive state is almost linear, i.e. the value of the resistance of the constriction is not affected by the flowing current when $I_{C,C} < I_B$. Both these aspects are very important to operate the strips in the regime where the constriction remain resistive all the time and the value of the resistance is only slightly affected from the current dynamics in the strip. The constriction behaves as an ideal resistor.

We also note that, for the strip connected to the $10 \times 10\,\mu\mathrm{m}^2$ thermal buffer, the ratio of $I_{C,S}/I_{C,C} = 1.5$ (see inset figure 1(b)) is much lower than the value of the ratio $W/w = 4$ as instead expected for a uniform current distribution in the strip, like in our case where Λ_P is larger than both W and w. The observed value of $I_{C,S}/I_{C,C} = 1.5$ indicated that the critical current is not governed by the de-pairing mechanism [23]. The fact that both the constriction and the strip are made from the same material with the same thickness and both are connected to the wider regions with rounded corners of about 50 nm radius (see figure 2(a)) excludes the current crowding effect [24] from explaining the observed $I_{C,S}/I_{C,C}$. We note that this reduced scaling of the critical currents in thin and narrow Nb strips have been observed previously and attributed to the phenomenon of vortex penetration [25].

3. Experimental results

Following the previous results, we fabricated a specially-designed SSID test device and characterized it in terms of I–V characteristics and current distribution dynamics before and after detection events. The device is based on the same 40 nm thick Nb thin film used for the fabrication of the previous devices. The whole structure is defined by single-step EBL and RIE, and consists of 11 parallel strips. Every strip consists
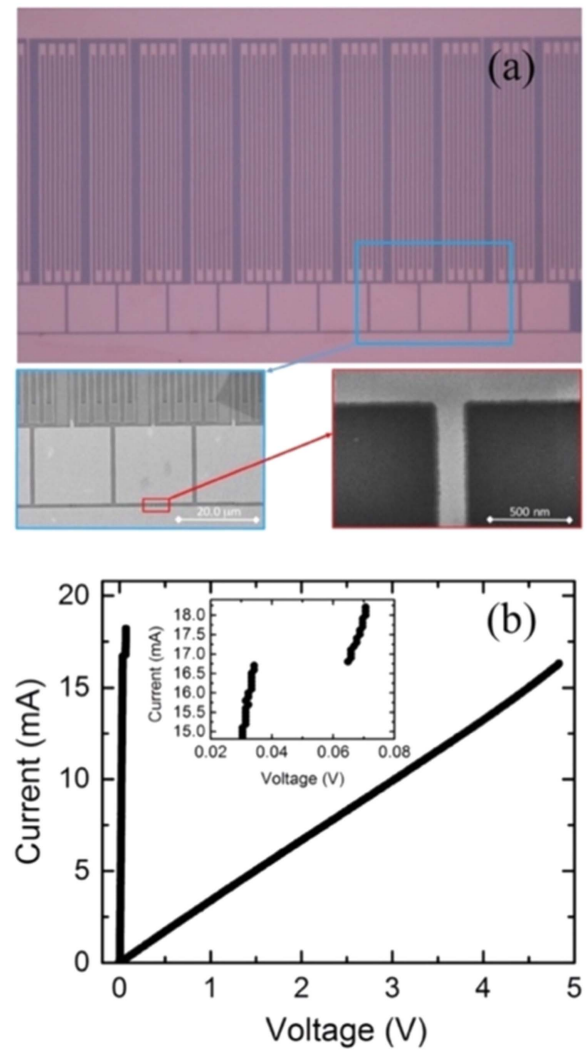
Figure 2. (a) Optical microscope image of the tested device (top) and SEM images at high magnification of the thermal buffers (bottom left) and nanowire (bottom right). (b) I–V characteristic of the fabricated device measured in a closed-cycle cryostat at $T = 3.7$ K.

of a meander with nine segments, each having $W = 1\,\mu$m, $L = 90\,\mu$m and a spacing of $1\,\mu$m (figure 2(a)). The meandered parallel strips are spaced by $\Delta x = 3.8\,\mu$m. On one side the strips are directly connected to a superconducting bank. On the other side each strip terminates with a superconducting thermal buffer having a size of $20 \times 20\,\mu\mathrm{m}^2$ at the end of which a constriction having width $w = 0.2\,\mu$m and length $l = 0.8\,\mu$m, connects the thermal buffer to another superconducting bank (figure 2(a)). In figure 2(b) we show the I–V characteristic of the fabricated device.

The realized device has a critical current of $I^{\mathrm{tot}}_{C,C} = 16.8\,\mathrm{mA}$ and $I^{\mathrm{tot}}_{C,S} = 18.3\,\mathrm{mA}$ at $T = 3.7$ K (figure 2(b)). The measured value of $I^{\mathrm{tot}}_{C,S}$ is much smaller than the expected value of about 29 mA. This reduced current may be due to an overheating effect between the resistive constrictions on the same side of the common superconducting bank that has a width of only $15\,\mu$m or could also arise from a non-uniformity of the strips. Nevertheless, the bias range

$I^{\text{tot}}{}_{\text{C,C}} < I_{\text{B}} < I^{\text{tot}}{}_{\text{C,S}}$ is sufficient to operate the device stably and to carry out investigations of current distribution.

In this study we employed an optical fiber-coupled miniature confocal microscope integrated in a closed-cycle pulse tube refrigerator [26]. The microscope optics are mounted on X, Y and Z piezoelectric motors, enabling the optical spot to be precisely aligned and brought into focus on the device. A 1550 nm diode laser beam was focussed to a spot size of $2.52 \pm 0.02\ \mu$m (full width at half maximum). This small size of the spot allows us to interact individually with each meandered line in the device. A fast electrical pulse generator was used to gain switch the laser diode creating short optical pulses sufficient to drive a region of the strip out of equilibrium and generate a measurable electrical output pulse [3, 4]. The output signal pulses were amplified using a 2 GHz bandwidth amplifier with a total gain of 30 dB and recorded on an 8 GHz bandwidth oscilloscope.

For the measurements, we centered the laser spot in the middle of each meandered strip in turn, referring to them as strip $i = 1$ to strip $i = 11$. As the ith strip generates a voltage pulse with an amplitude, A_i, that is proportional to the current flowing in the strip I_i, and $j_i = I_i/Wd$, we can write [3, 4]

$$\frac{A_i}{\sum_i A_i} = \frac{I_i}{\sum_i I_i} = \frac{J_i}{\sum_i J_i}, \tag{1}$$

where the sum on the index i is intended on all the $N = 11$ strips in the device. This equivalence allows us to infer the normalized current density in each strip by measuring the pulse amplitude generated when a laser pulse strikes it [3, 4].

In figure 3(a), we show the normalized current distribution obtained from the measurements using equation (1) (red squares) and the theoretical distribution obtained from the model of [3] for the same device with no resistor connected in series (black dots). The device is operated in the single strip switch regime [17] where when one strip is driven normal due to the laser pulse, the others remain in their superconducting state. Also, the constrictions remained resistive all the time during the detection events for the reasons mentioned before.

We see that the normalized current distribution is uniform (flat) and is completely different from the theoretical one used to fit the data in our previous experiments [3]. This means that the constrictions are acting as intended like resistors connected in series to the strips and the current effectively distributes uniformly in the parallel strips.

The observed small difference in the current distribution, is consequence of a non-uniformity in the fabrication of the constrictions, and thus of normal state resistances, that is bigger than the statistical spread of the measurements. In fact for a block of N current biased parallel strips, the variation of the flowing current with the value of the constriction's resistance $R_{\text{C},i}$ can be expressed as

$$\frac{dI_i}{I_i} \approx -\frac{dR_{\text{C},i}}{R_{\text{C},i}} = \frac{ds}{s}, \tag{2}$$

where s can be either the width or the thickness of the constriction; this equality is valid in the approximation of $N \gg 2$.
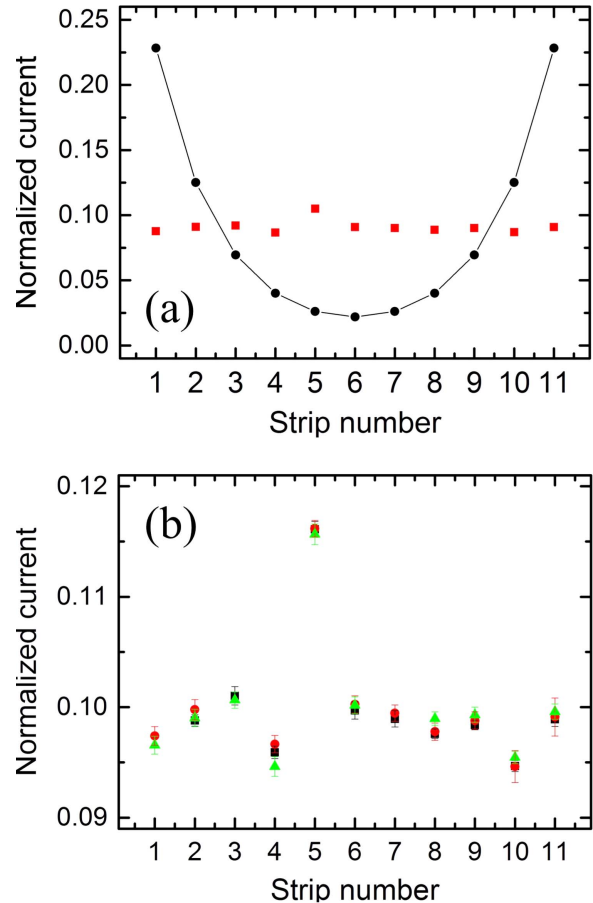
Figure 3. (a) Normalized measured (red squares) and calculated (black circle) current density as a function of the strip number. The calculated current density values are obtained by using the model of [3, 4] and a value for the parameter $a = 0.16$. (b) Measured normalized current pulse amplitudes as a function of the strip number values obtained when the strip 1 (black square), strip 3 (red circle) and strip 7 (green triangle) are struck.

Therefore, we can write:

$$\frac{dI_i}{\sum_i I_i} = \frac{ds}{s}\frac{I_i}{\sum_i I_i} = \frac{ds}{s}\frac{A_i}{\sum_i A_i}. \tag{3}$$

By considering the largest difference in the distribution of the normalized current values, between strip 2 and strip 10 in figure 3(a), we see that this implies a variation of only about 6%, corresponding to a 2.5 nm change in thickness or in a 12 nm change in the width of the constriction. Such variations are compatible with the obtainable resolution in the patterning of the device, performed with an old Crestec CABL9000 e-beam system with 30 kV acceleration voltage, and in the deposition of the thin films, done with a self assembled Material Research Corporation—MRC sputtering system. The value of strip 5 is clearly affected by a bigger defect out of the average in the fabrication. The variation of about 16%, corresponds to a 6.4 nm change in thickness or in a 32 nm change in the width of the constriction. In practice, it could be possible to observe this defect by carefully inspecting the sample by scanning electron microscope or by atomic force microscope, but the total length of the strip of about 1 mm could make the inspection time consuming.

4

To further investigate the effectiveness of this design, we measured also the current distribution after a first switching event using the *strike and probe* technique [4]. In our previous study, we showed that the occurring current re-distribution is strongly non-uniform in agreement with the generalized London model [4]. In figure 3(b) we show the normalized currents flowing in all the strips after strip $i = 1, 3$ and 7 have been struck with a laser pulse. The resulting current distributions are uniform within the statistical error of the measurements, irrespective of which strip was initially struck. As expected, the results with our new device are completely different from those observed in our previous studies with a conventional SSID device architecture [3, 4], where a strongly non-uniform current re-distribution with a shape depending on the position of the strips i in the device was seen.

4. Conclusions

We have realized and tested a device using an innovative parallel strip design to control the current dynamics. The design uses the bi-stable nature of a superconducting film, resistive or superconducting depending if the flowing current if bigger or smaller than the critical current, to form identical resistors connected in series with each strip and to break the superconducting loops avoiding magnetic flux trapping. This results in a stable uniform current distribution across the strips, governed by Ohm's law.

This design addresses the pressing problem of non-uniform current distributions occurring in parallel configuration SSIDs [3, 4] which is the main reason for the degradation of the detection efficiency and instability of operation [20]. Therefore, it will be possible to realize high efficiency SSID having the required area of about $1 \, \text{cm}^2$ by increasing the number of parallel strips at a suitable value to not slow down the response time of the detector [10]. This can be accomplished by designing a larger conducting bank connecting the parallel strips, to prevent the reducing of the critical current in the strips observed in our experiment, and considering that each constriction will dissipate a maximum power of only about $P_{\text{diss}} = (I^{\text{tot}}_{\text{C,S}})^2 \times V = 23 \, \mu\text{W}$ for the 40 nm thick Nb film. The standard power cooling of a cryostat at 4 K is about 0.2 W and therefore also for 100 parallel constrictions the dissipated power of $P_{\text{diss}} = 2.3 \, \text{mW}$ is only about 10% of the power cooling and the operation temperature can be easily maintained. Moreover, the value of power dissipation for each individual constriction can be further reduced by either (1) decreasing the length of constrictions, provided that he constriction will still operate in the resistive state all the time with $I_{\text{ret,S}} < I_{\text{ret,c}}$, or (2) increasing the thickness of the film, that in turn will also increase the detection efficiency as reported in [18]. The value of the resistance of the constriction, R_{c}, will have only a modest beneficial effect in reducing the characteristic time response $t_{\text{rise}} \simeq \dfrac{L_{\text{S}}}{NR_{\text{L}} + R_{\text{c}} + R_{\text{h}}}$ and the fall time $\tau_{\text{fall}} \simeq \dfrac{L_{\text{S}}}{NR_{\text{L}} + R_{\text{c}}}$ of the output pulse [10, 19], where N

is the number of parallel wires in the device, $R_{\text{L}} = 50 \, \Omega$ of the load impedance (oscilloscope, counter.) and R_{h} is the resistance of the hotspot generated in the fired strip. In our experiments $N \, R_{\text{L}} = 550 \, \Omega \gg R_{\text{c}} \simeq 29 \, \Omega$.

This study has significant potential impact in accelerating the development of next generation superconducting strip sensors for time of flight mass spectrometry. We plan to follow up this study with practical implementations of this detector architecture in SSID devices. Moreover, the physical insights from this study are of relevance to practical developments of superconducting technologies for single photon counting [6, 7] and superconducting electronics applications [27] as well.

ORCID iDs

A Casaburi ⓘ https://orcid.org/0000-0001-8684-3217
M Ejrnaes ⓘ https://orcid.org/0000-0002-7461-9143
M Ohkubo ⓘ https://orcid.org/0000-0002-2460-6387

References

[1] Orlando T P and Delin K A 1991 *Foundations of Applied Superconductivity* (Reading, MA: Addison-Wesley)
[2] Pearl J 1964 *Appl. Phys. Lett.* **5** 65
[3] Casaburi A, Heath R M, Tanner M G, Cristiano R, Ejrnaes M, Nappi C and Hadfield R H 2013 *Appl. Phys. Lett.* **103** 013503
[4] Casaburi A, Heath R M, Ejrnaes M, Nappi C, Cristiano R and Hadfield R H 2015 *Phys. Rev.* B **92** 214512
[5] Cristiano R, Ejrnaes M, Casaburi A, Zen N and Ohkubo M 2015 *Supercond. Sci. Technol.* **28** 124004
[6] Gol'tsman G N, Okunev O, Chulkova G, Lipatov A, Semenov A, Smirnov K, Voronov B, Dzardanov A, Williams C and Sobolewski R 2001 *Appl. Phys. Lett.* **79** 705
[7] Natarajan C M, Tanner M G and Hadfield R H 2012 *Supercond. Sci. Technol.* **25** 063001
[8] Ejrnaes M, Cristiano R, Quaranta O, Pagano S, Gaggero A, Mattioli F, Leoni R, Voronov B and Gol'tsmann G 2007 *Appl. Phys. Lett.* **91** 262509
[9] Tarkhov M *et al* 2008 *Appl. Phys. Lett.* **92** 241112
[10] Casaburi A, Zen N, Suzuki K, Ejrnaes M, Pagano S, Cristiano R and Ohkubo M 2009 *Appl. Phys. Lett.* **94** 212502
[11] Semenov A D, Gol'tsmann G N and Korneev A A 2001 *Physica* C **351** 349
[12] Suzuki K, Shiki S, Ukibe M, Koike M, Miki S, Wang Z and Ohkubo M 2011 *Appl. Phys. Express* **4** 083101
[13] Kerman A J, Yang J K W, Molnar R J, Dauler E A and Berggren K K 2009 *Phys. Rev.* B **79** 100509(R)

[14] Annunziata A *et al* 2010 *J. Appl. Phys.* **108** 084507

[15] Casaburi A, Heath R M, Tanner M G, Cristiano R, Ejrnaes M, Nappi C and Hadfield R H 2014 *Supercond. Sci. Technol.* **27** 044029

[16] Zen N, Miki S, Ukibe M, Koike M and Ohkubo M 2014 *Appl. Phys. Lett.* **104** 012601

[17] Casaburi A, Esposito E, Ejranes M, Suzuki K, Ohkubo M, Pagano S and Cristiano R 2012 *Supercond. Sci. Technol.* **25** 115004

[18] Casaburi A, Ejrnaes M, Zen N, Ohkubo M, Pagano S and Cristiano R 2011 *Appl. Phys. Lett.* **98** 023702

[19] Zen N, Casaburi A, Shiki S, Suzuki K, Ejrnaes M, Cristiano R and Ohkubo M 2009 *Appl. Phys. Lett.* **95** 172508

[20] Zen N, Fujii G, Shiki S, Ukibe M, Koike M and Ohkubo M 2015 *Chin. Phys.* B **24** 098501

[21] Skocpol W J, Beasley M R and Tinkam M 1974 *J. Appl. Phys.* **45** 4054

[22] Gray K E, Kampwirth R T, Zasadzinski J F and Ducharme S P 1983 *J. Phys. F: Met. Phys.* **13** 405

[23] Ilin K, Siegel M, Engel A, Bartolf H, Schilling A, Semenov A and Hubers H W 2008 *J. Low Temp. Phys.* **151** 585

[24] Hortensius H L, Driessen E F C, Klapwijk T M, Berggren K K and Clem J R 2012 *Appl. Phys. Lett.* **100** 182602

[25] Il'in K, Rall D, Siegel M, Engel A, Schilling A, Semenov A and Huebers H-W 2010 *Physica* C **470** 953

[26] Hadfield R H, Dalgarno P A, Ramsay E, Warburton R J, Gansen E J, Baek B and Nam S 2007 *Appl. Phys. Lett.* **91** 241108

[27] McCaughan A M and Breggren K K 2014 *Nano Lett.* **14** 5748